**ACTA IMEKO**
**ISSN: 2221-870X**
*March 2023, Volume 12, Number 1, 1 - 6*

# First experimental tests on the prototype of a capacitive oil level sensor for aeronautical applications

**Filippo Attivissimo[1], Francesco Adamo[1], Luisa De Palma[1], Daniel Lotano[1], Attilio Di Nisio[1]**

[1] *Dept. of Electrical and Information Engineering, Polytechnic University of Bari, Via Edoardo Orabona 4, I-70126 Bari, Italy*

ABSTRACT
In this paper, the design, the prototyping, and the first results of experimental tests of a Capacitive Oil Level Sensor (CLS) intended for aeronautical applications are described. Due to potentially high vibrational stresses and the presence of high electromagnetic interferences (EMI), the working conditions on aircraft can be considered quite harsh. Hence, both the sensing part and the conditioning circuit should meet strict constraints. For this reason, in the design phase, great attention has been paid also to the mechanical characteristics of the probes. All the design aspects are exposed and the main advantages concerning alternative level sensing techniques are discussed, and the preliminary experimental results of sensitivity, linearity, hysteresis, and settling time tests are presented and commented.

**Section:** RESEARCH PAPER

**Keywords:** Level sensor; CLS; helical; airborne; capillary effect; conditioning circuit

**Citation:** Filippo Attivissimo, Francesco Adamo, Luisa De Palma, Daniel Lotano, Attilio Di Nisio, First experimental tests on the prototype of a capacitive oil level sensor for aeronautical applications, Acta IMEKO, vol. 12, no. 1, article 27, March 2023, identifier: IMEKO-ACTA-12 (2023)-01-27

**Section Editor:** Francesco Lamonaca, University of Calabria, Italy

**Received** February 3, 2023; **In final form** February 16, 2023; **Published** March 2023



**Funding:** This research was funded by the Italian Ministry of University and Research (MUR) on the "PON R&I 2014-2020 – Area di specializzazione "Aerospazio", Project "FURTHER".

**Corresponding author:** Francesco Adamo, e-mail: francesco.adamo@poliba.it

## 1. INTRODUCTION

Aircrafts require highly reliable level monitoring for fluids like lubricant oils for the main engine as well as for other mechanical subsystems. These levels can be sensed using microwave sensors [1]-[4], TDR-based (Time Domain Reflectometry) sensors [5]-[6], optical sensors, and many other methods. However, these techniques usually require very complex and expensive signal conditioning hardware. Moreover, it is important to note that level monitoring in aeronautical applications requires a continuous measurement over the entire dynamic range. A Capacitive Level Sensor (CLS) perfectly fits this requirement because its output is not only continuous but even highly linear. A CLS carries even more benefits, as it needs a limited planned maintenance, has long MTBF (Mean Time Between Failures) and most importantly, it requires low-cost conditioning electronics.

Capacitive sensors are commonly used in a large variety of industrial applications for measuring several parameters, e.g., pressures, mechanical strains, displacements, ECG signals, facial movements, sound levels, fluid levels, object presence, and many others [7]-[18]. This paper investigates a novel approach to the design of a capacitive sensor for level sensing, with the proposal of a new geometry design for the sensing probes. The design is presented in section 2, starting from the work presented in [19]. Several problems will be discussed, such as vibrational stresses and capillarity effects of the fluid in the gap between probes.

In section 3 the details of the conditioning circuit (already presented in the previous paper [20]), the readout electronic and the test methodology will be discussed.

Finally, in section 4 the preliminary experimental results of the characterization of the prototypes will be provided.

## 2. SENSOR PROBES DESIGN

To develop a new sensor for lubricant oil level monitoring for aerospace applications, a first look at the "standard" or "conventional design" CLS probes is needed.

For reference purposes, we have considered the commercially available CLS model 8TJ209 from Ametek Aerospace [21]; it is made of two cylindrical and concentric metallic plates with a gap of about 4.3 mm and has a declared sensitivity of about $8\ \mathrm{pF/inch} \cong 315\ \mathrm{pF/m}$. Due to the relatively wide gap between plates, the dynamic response to a step variation of the

liquid level is of the second order, and thus prone to oscillations, as demonstrated in [22] and explained in the following. The aim of the novel design here presented is to increase the sensitivity and, at the same time, to improve the dynamic response reducing the overshoot and the settling time.

The sensitivity of a CLS is simply defined as the first partial derivative of the output capacitance vs. the liquid level: $S \stackrel{\text{def}}{=} {\vartheta C}/{\vartheta h}$. In working conditions these kinds of CLSs can be seen as the parallel connection of two capacitors: the first one corresponding to the section immersed into the liquid and the second one corresponding to the remaining section where the dielectric is the air; so the total output capacitance is given by:

$$C = \frac{C_0}{L}\left[\varepsilon_{r,liq} \cdot h + (L - h)\right], \tag{1}$$

where $h$ is the liquid level, $L$ is the length of the probe, $\varepsilon_{r,liq}$ is the relative permittivity of the sensed liquid and, finally, $C_0$ is the "dry capacitance" of the sensor, i.e. the capacitance shown at the output terminals when the fluid level is $h = 0$. For simplicity, it has been assumed that relative permittivity of air is one. Following the definition of sensitivity, we can write:

$$S = \frac{C_0}{L}\left(\varepsilon_{r,liq} - 1\right). \tag{2}$$

Equations (1) and (2) are generic and can be adapted to CLSs with concentric cylindrical armatures simply considering that for this kind of geometry the dry capacitance per unit length ${C_0}/{L}$ is given by:

$$\frac{C_0}{L} = \frac{2\pi\varepsilon_0}{\ln\frac{r_e}{R_i}} = \frac{2\pi\varepsilon_0}{\ln\frac{1}{1-\frac{w}{r_e}}}, \tag{3}$$

where $\varepsilon_0$ is the vacuum/air permittivity, $r_e$ is the inner radius of the external electrode, $R_i$ is the outer radius of the internal electrode and $w = r_e - R_i$ is the gap between the electrodes.

From equations (2) and (3) it's easy to see that the sensitivity $S$ increases when the ratio $w/r_e$ decreases or, in other words, when the gap $w$ between the electrodes is narrowed.

Narrowing the gap has also the additional effect of improving the dynamic response of the sensor, as the mechanical behaviour of the liquid in between the plates of the probe changes. In fact, performing numerical simulations for decreasing values of $w$, the dynamic response to a step input level changes from a second order one to a first-order approximation when $w \leq 1.35$ mm [22]. This result has been obtained by considering that the system is modelled by communicating vessels, and can be described by the second-order non-linear equation deeply investigated as equation (12) in the mentioned manuscript. The analysis takes into account several pressure variables, such as hydrostatic pressure, electrostatic pressure, pressure drop due to friction losses and so on.

Table 1. Sensitivities of the proposed CLS calculated in COMSOL Multiphysics®. Corresponding sensitivity concerning an uncut probe.

| Slit contour | Sensitivity (pF/m) |
|---|---|
| No slit | 725 |
| Helicoidal | 718 |
| Straight | 723 |

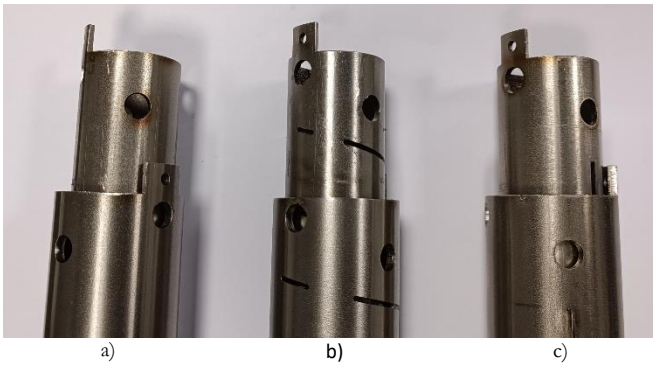

a) b) c)

Figure 1. Electrodes prototypes used in the experiments: a) without slits b) with helical slits and b) with a longitudinal straight slit.

However, some negative aspects must also be carefully considered: *i)* with such a marked gap-width reduction, a significant capillarity rise starts to happen, and *ii)* the oil is held on the plates for a longer period due to its viscosity.

The capillarity effect can be numerically modelled and addressed by engraving slits into at least one of the concentric probes so that no column above the bath level can build up in the channel. Two kinds of contour have been considered for the slits, as shown in Figure 1: helicoidal and straight. Both were carefully modelled and studied in COMSOL Multiphysics® to calculate the physical characteristics, in particular their sensitivities [22].

Furthermore, also the mechanical behaviour of these new kinds of electrodes was carefully studied. In fact, in the typical operating condition aboard helicopters, the vibrational stresses are very significant, and, if not modelled and counteracted the resulting behaviour of the sensor could be undetermined. In fact, in presence of intense mechanical vibrations, the electrodes are set in relative motion to each other, so capacitance fluctuations and, at least potentially, also possible short circuits can occur.

The highest values of vibration frequencies occur on helicopters with many blades in the main rotor. As an example, consider a rotor with 7 blades spinning at 225 rpm; in these conditions, the fundamental excitation frequency is $f = 225 \cdot {7}/{60} \cong 25$ Hz. It is then important that the vibrational modes of the proposed probes have higher frequencies than the ones occurring on the helicopter where it is used. For our analysis, only the flexural vibrations were considered, because longitudinal and torsional ones do not alter the relative position of the electrodes due to the mechanical constraints [22]. Due to this constraint as well as to the chemically highly aggressive environment in which the sensor must work, we choose to make the probe prototypes in marine-grade stainless steel (AISI-316); materials like copper or bronze have been excluded a-priori due to their poor resistances to corrosion phenomena [23]-[24].

Performing a FEM (Finite Elements Method) analysis of the modes of vibration, the probe with the longitudinal slit shows the lowest resonant frequencies at 67 Hz for the internal electrode and 83 Hz for the external electrode, while the resonant frequencies for the helicoidal slit probe are 37 Hz and 44 Hz respectively. Hence, both probes have higher modes than the vibrations on the helicopter, so no resonances will occur in working conditions.

After these preliminary considerations, three different probes were manufactured and tested: one with a helicoidal slit, one with a straight longitudinal slit, and a third one with the internal electrode without any cut and the external electrode with the same previous helical slit.


Figure 2. The prototype of the sensor readout electronics based on the FDC2214.

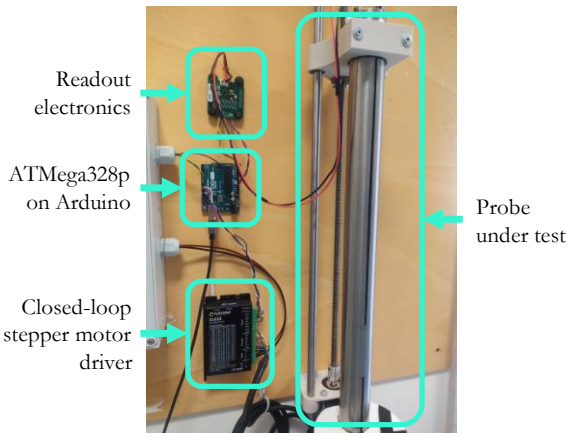


Figure 3 . The mechatronic system developed for the automated tests on the CLS prototypes; the four main parts of the system are evidenced.

## 3. EXPERIMENTAL SETUP AND METHODS

The purposely designed and prototyped readout electronics as well as the methodology followed for the experiments and the sampling of the data is explained in the following. A look at the mechatronic setup used for the sliding of the probes in and out of the oil is given too.

### 3.1. Conditioning circuit

One of the most common and immediate ways to measure the output capacitance of a capacitive sensor is to insert it in a low-pass series RC filter and then measure its time constant in response to a step voltage input stimulus. In such a circuit, the current is given by:

$$i(t) = \frac{V}{R} e^{-\frac{t}{\tau}}, \tag{4}$$

where $\tau = R\,C$ is the time constant. Hence, the capacity can be calculated by measuring the time needed to charge the capacitor through the resistor from a given start voltage to an end voltage. Unfortunately, this method is unreliable because of two main reasons: 1) the effective resolution of low-cost ADCs or even of the ADCs integrated into typical microcontrollers is too low (typically less than 12 bits) to achieve the requested measurement accuracy, and 2) the time needed to complete a measurement can be too long.

In this work a different approach was pursued: we used an LC tank oscillator circuit for the measurement of the frequency shift due to capacitance variations. A parallel LC oscillator has a well-known resonant oscillation frequency where the capacitor reactance matches the inductor reactance:

$$X_{C_{\mathrm{tot}}} = \frac{1}{2\,\pi\,f\,C_{\mathrm{tot}}} = 2\,\pi\,f\,L = X_L\,, \tag{5}$$

where:

- $X_{C_{\mathrm{tot}}}$ and $X_{\mathrm{L}}$ are the capacitor and the inductor reactance respectively.
- $C_{\mathrm{tot}}$ is the total capacitance in the circuit, i.e. the sum of a fixed capacity value $C$ and of the sensor's capacitance $C_x$; to improve the measurement accuracy, also the parasitic capacitances $C_{\mathrm{par}}$ due to the printed circuit board (PCB) traces and to the connecting cables must be included.
- $L$ is the inductance in the oscillator circuit and $f$ is the resonant frequency.

Equation (5) can be rewritten with the resonant frequency on the left-hand side as:

$$f = \frac{1}{2\,\pi\,\sqrt{L\,C_{\mathrm{tot}}}}. \tag{6}$$

Hence the sensor's capacitance $C_x$ can be calculated from (6) as:

$$C_x(f) = \frac{1}{L(2\,\pi\,f)^2} - \left(C + C_{\mathrm{par}}\right). \tag{7}$$

The tank oscillator was implemented using standard commercial values for inductor $L$ and capacitor $C$, namely $L = 10\ \mu\mathrm{H}$ and $C = 270\ \mathrm{pF}$. The PCB parasitic capacitance was measured to be $C_{\mathrm{par}} \cong 13\ \mathrm{pF}$, i.e. a value well in line with typical mean values of capacitance on a PCB. If we assume that the sensor's capacitance spans the range 500 nF – 1000 pF, the expected frequency span is about 393 kHz.

### 3.2. Measurement system

The sensor readout is performed by the FDC2214 by Texas Instruments, a specialized capacitance-to-frequency converter (CFC) integrated circuit (IC) [25]-[27]. The FDC2214 was selected among many alternative ICs because it has 4 independent input channels with a full-scale range (FSR) of up to 250 nF, a nominal resolution of 28 bits, an RMS noise of 0.3 fF, and an output data rate of 4.08 kSa/s. The prototype of the PCB with the FDC2214 and the minimum electronics needed to interface it with an external microcontroller is shown in Figure 2.

The FDC2214 communicates with the external microcontroller through an I2C (Inter Integrated Circuits) interface. To interface it with a PC, we used a simple Arduino Uno development system with an ATMega328p MCU (Micro Controller Unit) by Microchip Corp. Measurement data are acquired from the FDC2214 by the MCU and transferred to the PC where they are processed in MathWorks MATLAB.

To simplify the test procedures, the probes being characterized were tied to a high-precision linear actuator and suspended over a 125 mm diameter PVC pipe filled with lubricant oil (Figure 3). The probes were mounted on the moving cart of the system driven by a closed-loop controlled stepper motor and a high-precision trapezoidal screw. This setup allowed the positioning of the sensor with a nominal resolution of 50 µm.

For the sake of completeness, it must be said that this setup has been preferred to the one on which the sensor probes are set

in position in a tank and a pump is used to fill and empty the tank with the lubricant oil, due to the limited maximum flow of the available pumps.

The lubricant oil used for the tests is an SAE 15W40 standard, semi-synthetic one by Viskoil®. Its characteristics were deeply studied and described in [28]. Some assumptions for the experimental tests were done:

- the room temperature in the laboratory was considered constant.
- the lubricant is not worn as it is not working in a motor, so there is no contamination by water nor coolant, or metallic debris.

From [28], the dielectric constant reduces by only 1.5% when the temperature rises from 60 °C to 120 °C; so, in a first approximation, its changes can be considered linear in the working temperature range of a typical high-performance aeronautical motor (about 100 °C). In the following, the relative dielectric constant is assumed to be $\varepsilon_{r,oil} = 2.2$.

In perspective, the effects of temperature on the dielectric constant could also be measured and compensated by taking advantage of one of the residual 3 channels available on the FDC2214; in fact, it can be used to measure the capacitance of a reference capacitor with known geometry permanently and fully immersed in the same oil tank where the CLS is installed.

### 3.3. Test methods

For each sensor, sensitivity, hysteresis, rise time, and root mean square non-linearity error (RMSE) have been studied and evaluated to carry out a comparison.

Hysteresis experiments were done with three immersion and extraction cycles of the probes with increasing pause times between the moving and the sampling phase. The experiments were performed over a full run of 400 mm in 10 mm steps. For each step, after a delay time (if added), 100 samples were taken in a time interval of about 2 s. The mean absolute hysteresis is calculated as the mean of the differences between the immersion and extraction measures. The sensitivity is calculated by fitting the 10 s cycle data with a first-grade polynomial function.

The rise time experiments were performed by measuring the sensor's output capacitance for a minimum of 20 s, after rapidly dipping or extracting the probe into/from the oil. The time constant $\tau_{63}$ was calculated as 63 % of the time from the moment the sensor stopped to the moment its output capacitance reached its settled value. Settling time was then assumed to be $t_r = 5 \cdot \tau_{63}$.

The same sampled data were also used to calculate the sensitivity of the sensor and the RMSE, both for the immersion and for the extraction movements.

Table 2. Comparison of performances of the CLS with the three different kinds of electrodes

| Probe | Sensitivity pF/mm | $Max\ \lvert NLE \rvert^{(*)}$ pF | $Max\ \lvert hysteresis \rvert$ pF | Rise time s |
|---|---|---|---|---|
| Helicoidal | 0.949 | 4.59 | 2.57 | 4.85 |
| Mixed | 0.888 | 1.93 | 1.24 | 3.01 |
| Straight | 0.879 | 11.58 | 5.10 | 3.01 |

(*) NLE = Non-Linearity Error

## 4. RESULTS

According to the hysteresis experiment, the sensor with mixed electrodes, i.e., the probe with the internal plate without slits and the external plate with helicoidal slits, showed overall the least residual non-linearity. With respect to this aspect, when given enough time for the settling of the output capacitance, the longitudinal slit probe appears to be the worst-performing one. The sensitivity shown by all the sensors is about 25% higher than the one expected from the simulations run in COMSOL Multiphysics®. The highest sensitivity was achieved with the helicoidal slits probe: this is not in accordance with the physics and could be due to a misalignment of plates or to the small defects of the manufacturing process. Other prototypes of the electrodes will be prepared but with different and more accurate manufacturing processes to study this phenomenon.

With respect to the rise time evaluation experiments, the main issues arose with the helicoidal probe; in fact, in this case, we observed a very high $\tau_{63}$ time constant since *i)* the gap between the two electrodes is very narrow and this, as already explained, increases the time needed for the oil to rise and fall in the gap, and *ii)* the slits are narrow too, allowing a thin membrane of oil to form in them. Hence, the oil is held on the electrodes for a longer time. Moreover, the time constants are different for increasing and decreasing oil levels; indeed, the time constant is higher for the extraction paths due to the oil retention phenomenon. In this case, the vertical slit electrodes performed best, even though the results are comparable to the mixed electrodes ones.

Finally, a preliminary look was given at the dynamic performance of the sensors. The residual non-linearity RMSE is comparable for all three probes. Results for the immersion and extraction are similar too. However, when fitting the sampled data and calculating the sensitivity, a clear difference between the extraction and immersion characteristics arises, with the sensitivity for the immersion being lower than the extraction.

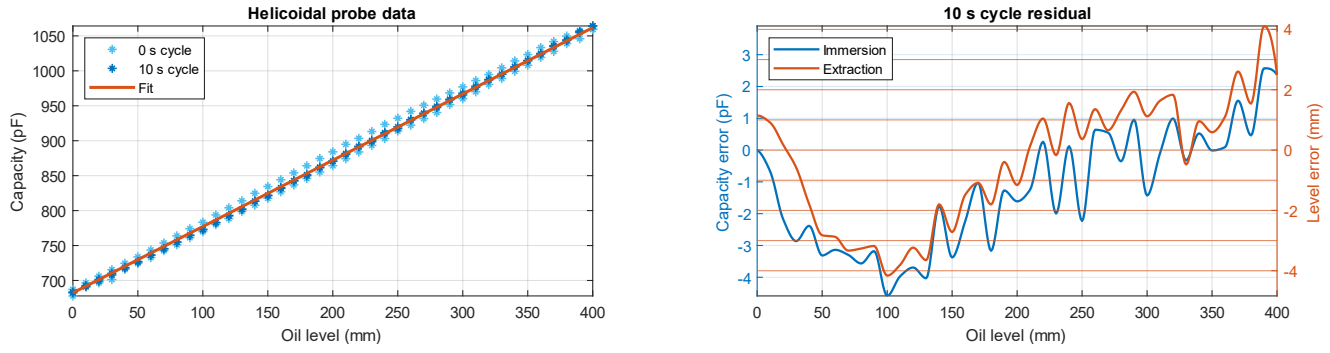


Figure 4. Results of the hysteresis experiment on probes with helicoidal slits a) linear fit and b) residuals.

## 5. CONCLUSIONS

In this manuscript, the authors presented a novel design strategy for oil-level monitoring aboard aircraft. After a first in-depth study of a novel geometry for the probes, with accurate numerical simulations on the electrical aspects, also the effects of mechanical stresses on the electrodes were modelled and addressed. The probes have been prototyped and tested using an in-house developed PC-based mechatronic system and readout electronic.

The tests showed positive results in line with the expected behaviour predicted through simulations. In particular, the proposed solution proved superior to the other level sensing technologies in the industry nowadays. Concerning the sensitivity, the proposed sensor showed an improvement of more than three times with respect to other commercial CLSs. Furthermore, the issue of the second-order response in response to a step change in the oil level was overcome, with an improvement in the settling time too.

Even the comparison with an optical level sensor is promising, as the readout electronic is simpler, cheaper, and most important more reliable.

The readout electronic was prototyped in a small series with a cost of about 50 EUR/unit while, the cost of a single set of probes of the CSL is around 1,500 EUR, due to the complexities of the manufacturing process. Of course, both these cost components could be reduced in the mass production of the sensor. However, it can be estimated that also with a limited number of units the overall cost of the proposed system could be lower than that of the corresponding optical or microwave solutions.

## ACKNOWLEDGEMENT

This study has been developed in close cooperation with an international aerospace company within the Project FURTHER "Future Revolutionary Technologies for Hybrid Electric Aircrafts", funded by the Italian Ministry of University and Research (MUR) through the research program PON R&I 2014-2020.

## REFERENCES

[1] M. Vogt, C. Schulz, C. Dahl, I. Rolfes, M. Gerding, An 80 GHz radar level measurement system with dielectric lens antenna, 2015 16th International Radar Symposium (IRS), Dresden, Germany, 24-26 June 2015, pp. 712-717.
DOI: 10.1109/IRS.2015.7226222

[2] Kunde Santhosh Kumar, A. Bavithra, M. Ganesh Madhan, A cavity model microwave patch antenna for lubricating oil sensor applications, Materials Today: Proceedings, vol. 66, Part 8, 2022, pp. 3446-3449.
DOI: 10.1016/j.matpr.2022.06.136

[3] A. M. Loconsole, V. V. Francione, V. Portosi, O. Losito, M. Catalano, A. Di Nisio, F. Attivissimo, F. Prudenzano, Substrate-Integrated Waveguide Microwave Sensor for Water-in-Diesel Fuel Applications, Applied Sciences, vol. 11, 2021, no. 21, art. no. 10454.
DOI: 10.3390/app112110454

[4] G. Andria, F. Attivissimo, S. M. Camporeale, A. Di Nisio, P. Pappalardi, A. Trotta, Design of a Microwave Sensor for Measurement of Water in Fuel Contamination, Measurement, vol. 136, 2019, pp. 74-81.
DOI: 10.1016/j.measurement.2018.12.076

[5] M. Scarpetta, M. Spadavecchia, F. Adamo, M.A. Ragolia, N. Giaquinto, Detection and Characterization of Multiple Discontinuities in Cables with Time-Domain Reflectometry and Convolutional Neural Networks., Sensors, vol. 21, 2021, no. 23, 8032, 13 pp.
DOI: 10.3390/s21238032

[6] M. Scarpetta, M. Spadavecchia, G. Andria, M. A. Ragolia, N. Giaquinto, Analysis of TDR Signals with Convolutional Neural Networks, Proc. of IEEE Int. Instrumentation and Measurement Technology Conference (I2MTC), Glasgow, United Kingdom, 17-20 May 2021, pp. 1-6.
DOI: 10.1109/I2MTC50364.2021.9460009

[7] X. X. Liu, K. Peng, Z. Chen, H. Pu, Z. Yu, A New Capacitive Displacement Sensor with Nanometer Accuracy and Long Range, IEEE Sensors Journal, vol. 16, 2016, no. 8, pp. 2306-2316.
DOI: 10.1109/JSEN.2016.2521681

[8] M.-Y. Cheng, C.-L. Lin, Y.-T. Lai, Y. J. Yang, A Polymer-Based Capacitive Sensing Array for Normal and Shear Force Measurement, Sensors, vol. 10, 2010, no. 11, pp. 10211-10225.
DOI: 10.3390/s101110211

[9] A. Ueno, Y. Akabane, T. Kato, H. Hoshino, S. Kataoka, Y. Ishiyama, Capacitive Sensing of Electrocardiographic Potential Through Cloth from the Dorsal Surface of the Body in a Supine Position: A Preliminary Study, IEEE Transactions on Biomedical Engineering, vol. 54, 2007, no. 4, pp. 759-766.
DOI: 10.1109/TBME.2006.889201

[10] V. Rantanen, P. Kumpulainen, H. Venesvirta, J. Verho, O. Špakov, J. Lylykangas, A. Vetek, V. Surakka, J. Lekkala, Capacitive facial activity measurement, Acta IMEKO, vol. 2, 2013, no. 2, pp. 78-85.
DOI: 10.21014/acta_imeko.v2i2.121

[11] M. A. Ragolia, A. M. Lanzolla, G. Percoco, G. Stano, A. Di Nisio, Thermal Characterization of New 3D-Printed Bendable, Coplanar Capacitive Sensors, Sensors, vol. 21, 2021, art. no. 6324.
DOI: 10.3390/s21196324

[12] G. Stano, A. Di Nisio, A. M. Lanzolla, M. A. Ragolia, G. Percoco, Additive manufacturing for capacitive liquid level sensors, The International Journal of Advanced Manufacturing Technology, vol. 123, no. 7, 2022, pp. 2519–2529.
DOI: 10.1007/s00170-022-10344-7

[13] Q. Yang, A. J. Yu, J. Simonton, G. Yang, Y. Dohrmann, Z. Kang, Y. Li, J. Mo, F.-Y. Zhang, An inkjet-printed capacitive sensor for water level or quality monitoring: Investigated theoretically and experimentally, Journal of Materials Chemistry A, vol.5, 2017, 17841–17847.
DOI: 10.1039/C7TA05094A

[14] R. N. Miles, W. Cui, Q. T. Su, D. Homentcovschi, A MEMS Low-Noise Sound Pressure Gradient Microphone with Capacitive Sensing, Journal of Microelectromechanical Systems, vol. 24, 2015, no. 1, pp. 241-248.
DOI: 10.1109/JMEMS.2014.2329136

[15] N. L. Buck, R. A. Aherin, Human presence detection by a capacitive proximity sensor, Applied Engineering in Agriculture, vol. 7, 1991, no. 1, pp. 55-60.
DOI: 10.13031/2013.26191

[16] G. Stano, A. Di Nisio, A.M. Lanzolla, M. Ragolia, G. Percoco, Fused filament fabrication of commercial conductive filaments: experimental study on the process parameters aimed at the minimization, repeatability and thermal characterization of electrical resistance, The International Journal of Advanced Manufacturing Technology, vol. 111, 2020, pp. 2971-2986.
DOI: 10.1007/s00170-020-06318-2

[17] Texas Instruments, Common Inductive and Capacitive Sensing Applications (Rev. B), 2021. Online [Accessed 26 February 2023] https://www.ti.com/lit/pdf/slya048

[18] Texas Instruments, Accurate frost or ice detection based on capacitive sensing, 2018. Online [Accessed 26 February 2023] https://e2e.ti.com/blogs_/b/industrial_strength/posts/accurate-frost-or-ice-detection-based-on-capacitive-sensing

[19] L. De Palma, F. Adamo, F. Attivissimo, S. de Gioia, A. Di Nisio, A. Lanzolla, M. Scarpetta, Low-cost capacitive sensor for oil-level monitoring in aircraft, Proc. of IEEE Int. Instrumentation and

Measurement Technology Conference (I2MTC), Ottawa, ON, Canada, 16-19 May 2022, pp. 1-4.
DOI: 10.1109/I2MTC48687.2022.9806667

[20] F. Adamo, F. Attivissimo, S. de Gioia, A. Di Nisio, D. Lotano, M. Savino, Development and Prototyping of a Capacitive Oil Level Sensor for Aeronautical Applications, Proc. of 25th IMEKO TC4 Int. Symposium, Brescia, Italy, 12-14 September 2022. Online [Accessed 26 February 2023] https://www.imeko.org/publications/tc4-2022/IMEKO-TC4-2022-61.pdf

[21] Ametek Aerospace, 8TJ209 Capacitive Level Sensor Data Sheet. Online [Accessed 26 February 2023] https://www.ameteksfms.com/-/media/ameteksensors/documents/sensor-data-sheets/8tj209-capacitive-oil-level-sensor.pdf

[22] F. Adamo, F. Attivissimo, S. de Gioia, D. Lotano, A. Di Nisio, A design strategy for performance improvement of capacitive sensors for in-flight oil-level monitoring aboard helicopters, Measurement, 2023, 112476.
DOI: 10.1016/j.measurement.2023.112476

[23] L. Iannucci, L. Lombardo, M. Parvis, P. Cristiani, R. Basseguy, E. Angelini, S. Grassini, An imaging system for microbial corrosion analysis, Proc. of IEEE Int. Instrumentation and Measurement Technology Conference, Auckland, New Zealand, 20-23 May 2019, pp. 1-6.
DOI: 10.1109/I2MTC.2019.8826965

[24] L. Iannucci, M. Parvis, P. Cristiani, R. Ferrero, E. Angelini, S. Grassini, A Novel Approach for Microbial Corrosion Assessment, IEEE Transactions on Instrumentation and Measurement, vol. 68, 2019, no. 5, pp. 1424-1431.
DOI: 10.1109/TIM.2019.2905734

[25] Texas Instruments, FDC2x1x EMI-Resistant 28-Bit,12-Bit Capacitance-to-Digital Converter for Proximity and Level Sensing Applications datasheet (Rev. A). Online [Accessed 26 February 2023] https://www.ti.com/lit/gpn/fdc2214

[26] Texas Instruments, Capacitive Sensing: Direct vs Remote Liquid Level Sensing Performance Analysis (Rev. A), 2015. Online [Accessed 26 February 2023] https://www.ti.com/lit/pdf/snoa935

[27] Texas Instruments, FDC2114 and FDC2214 EVM User's Guide, 2016. Online [Accessed 26 February 2023] https://www.ti.com/lit/ug/snou138a/

[28] H. Sun, Y. Liu, J. Tan, Research on Testing Method of Oil Characteristic Based on Quartz Tuning Fork Sensor, Applied Sciences, vol. 11, 2021, no. 12, p. 5642.
DOI: 10.3390/app11125642